

Joint Transportation Research Program

FHWA/IN/JTRP-2010/25

Safety Enhancement of the INDOT Network Pavement Friction Testing Program:

Macrotexture and Microtexture Testing Using Laser Sensors

By

Shuo Li, Ph.D., P.E.
Transportation Research Engineer
Division of Research and Development
Indiana Department of Transportation

Samy Noureldin, Ph.D., P.E.
Transportation Systems Section manager
Division of Research and Development
Indiana Department of Transportation

And

Karen Zhu, Ph.D.
Senior System Analysts
Division of Research and Development
Indiana Department of Transportation

Joint Transportation Research Program
Project No. C-36-31V
File No. 02-11-22
SPR-3061

Prepared in Cooperation with the
Indiana Department of Transportation and the
U.S. Department of Transportation
Federal Highway Administration

The contents of this report reflect the views of the author who is responsible for the facts and the accuracy of the data presented herein. The contents do not necessarily reflect the official views or policies of the Indiana Department of Transportation or the Federal Highway Administration at the time of publication. This report does not constitute a standard, specification, or regulation.

Purdue University
West Lafayette, Indiana 47907
December, 2010

TECHNICAL REPORT STANDARD TITLE PAGE

1. Report No. FHWA/IN/JTRP-2010/25	2. Government Accession No.	3. Recipient's Catalog No.	
4. Title and Subtitle Safety Enhancement of the INDOT Network Pavement Friction Testing Program: Macrotecture and Microtexture Testing Using Laser Sensors		5. Report Date December, 2010	
		6. Performing Organization Code	
7. Author(s) Shuo Li, Samy Noureldin, and Karen Zhu		8. Performing Organization Report No. FHWA/IN/JTRP-2010/25	
9. Performing Organization Name and Address Joint Transportation Research Program 1284 Civil Engineering Building Purdue University West Lafayette, Indiana 47907-1284		10. Work Unit No.	
		11. Contract or Grant No. SPR-3061	
12. Sponsoring Agency Name and Address Indiana Department of Transportation State Office Building 100 North Senate Avenue Indianapolis, IN 46204		13. Type of Report and Period Covered Final Report	
		14. Sponsoring Agency Code	
15. Supplementary Notes Prepared in cooperation with the Indiana Department of Transportation and Federal Highway Administration.			
<p>16. Abstract</p> <p>The Indiana Department of Transportation has conducted annual network inventory friction testing using the locked wheel trailer to reduce wet pavement crashes. However, issues have arisen concerning the data credibility and field operation safety on high-speed highway facilities. Some researchers have investigated the evaluation of pavement friction using macrotecture measurements and found the relationship between friction and macrotecture is extremely weak. Currently, macrotecture can be readily measured at highway speeds, but microtexture is evaluated using friction at low speeds from a surrogate device. Microtexture plays an important role in friction force. The evaluation of pavement friction from texture measurements will be undermined without considering microtexture. This pilot study was conducted by the authors to examine the use of laser-based sensors in measuring pavement texture, in particular microtexture. The requirement for laser sampling frequency was established for choosing lasers during testing at highway speeds.</p> <p>Microtexture testing was conducted on cores taken from pavements. It was found that the Microtexture MPD, RMS and SV increased as the baseline length increased, regardless of the type of pavement, but tended to remain constant after the baseline length exceeded 12.75 mm. It was recommended that the microtexture MPD, RMS and SV should be computed in terms of a baseline length used for computing macrotecture. When estimating friction from microtexture measurements, the use of SV was as effective as the use of RMS. It is not necessary to include both SV and RMS when estimating friction from microtexture. Correlation analysis indicated that wet pavement friction had a positive relationship with macrotecture MPD, microtexture MPD, and microtexture SV. The microtexture SV may play a more important role in wet pavement friction than the microtexture MPD. Dry pavement friction is not as sensitive to macrotecture as to microtexture. Regression analysis indicated that pavement friction is related to both macrotecture and microtexture, not to macrotecture only. In addition, when pavement is wet, its surface friction is more sensitive to the slope variance than to the mean profile depth of the microtexture profile.</p> <p>It was recommended that more research effort is needed to investigate the characterization of microtexture and examine the effect of macrotecture slope variance. Research work is also needed to examine the image processing technology for measuring microtexture, and to confirm the hypothesis that pavement friction is probably related to microtextures with wavelengths greater than a certain value.</p>			
17. Key Words Weigh-in-motion, vehicle tracking, traffic monitoring, dynamic content based image segmentation, vehicle classification, infra-red light technology, weather condition		18. Distribution Statement No restrictions. This document is available to the public through the National Technical Information Service, Springfield, VA 22161	
19. Security Classif. (of this report) Unclassified	20. Security Classif. (of this page) Unclassified	21. No. of Pages 42	22. Price

TABLE OF CONTENTS

TABLE OF CONTENTS	i
LIST OF TABLES	ii
LIST OF FIGURES	iii
ACKNOWLEDGMENTS	iv
 <i>Chapter 1</i>	
INTRODUCTION	1
Problem Statement.....	1
Objectives.....	2
Scope of Work.....	3
 <i>Chapter 2</i>	
CHARACTERISTICS OF PAVEMENT SURFACE TEXTURE AND FRICTION	4
Surface Texture Characteristics.....	4
Quantitative Texture Measurements.....	6
 <i>Chapter 3</i>	
TEXTURE LASER SYSTEMS AND TEST SETUP	10
Selection of Texture Laser Measuring Systems.....	10
Pavement Texture Testing.....	14
 <i>Chapter 4</i>	
TEXTURE DATA ANALYSIS	17
Surface Macrotexture.....	17
Surface Microtexture.....	20
Measurement of Microtexture Properties.....	25
 <i>Chapter 5</i>	
POTENTIAL USE OF MICROTTEXTURE MEASUREMENTS IN ESTIMATING FRICTON	29
Pavement Friction Components.....	29
Comparison of Texture and Friction Measurements.....	30
Quantitative Relationship between Texture and Friction.....	35
 <i>Chapter 6</i>	
CONCLUSIONS AND RECOMMENDATIONS	37
Conclusions.....	37
Recommendations.....	39
 REFERENCES	 40

LIST OF TABLES

Table 3-1 Pavement Texture Frequencies by Wavelength at Different Speeds.....	11
Table 3-2 Laser System Specifications.....	13
Table 3-3 Friction Properties of the Friction Test Track Surfaces.....	14
Table 3-4 Comparison of MPD on Tined Concrete Surface.....	15
Table 3-5 Measurements of Macrotexture at Different Speeds.....	16
Table 4-1 Summary of MPDs Measured by Different Devices.....	19
Table 4-2 Summary of the Distributions of Microtexture Depth.....	23
Table 4-3 Summary of Microtexture Wavelength Statistics.....	25
Table 4-4 The MPD, SV, and RMS in Terms of 12.75-mm Baseline.....	28
Table 5-1 Friction Numbers Measured on Wet and Dry Pavement.....	30
Table 5-2 Friction Numbers under Different Pavement Conditions.....	31
Table 5-3 Pearson Correlations between Friction and Texture Measurements.....	35

LIST OF FIGURES

Figure 2-1 Texture Wavelengths and Impacts.....	5
Figure 2-2 Illustration of Texture Computation.....	6
Figure 3-1 Laser’s Sampling Frequency Required at Different Test Speeds.....	12
Figure 3-2 The 1 kHz Laser Texture Scanner.....	12
Figure 3-3 The 62.5 kHz Laser System Mounted on a Test Vehicle.....	13
Figure 3-4 INDOT Friction Test Track.....	14
Figure 3-5 MPD Values Measured at Different Time.....	15
Figure 4-1 Typical Macrottexture Profiles Measured Using 1 kHz and 62.5 kHz Lasers.....	18
Figure 4-2 Microtexture Profiles Measured on Three Surfaces.....	21
Figure 4-3 Typical Microtexture Profiles on Three Surfaces.....	22
Figure 4-4 Microtexture Profiles on a 1-mm Long Segment Surface.....	22
Figure 4-5 Distributions of Microtexture Depths on Three Surfaces.....	23
Figure 4-6 Example Plot for Manual Calculation of Wavelength.....	24
Figure 4-7 Microtexture Wavelength Distributions on Three Surfaces.....	25
Figure 4-8 Variations of MPD, SV, and RMS with Baseline Length.....	26
Figure 5-1 Surface of the Tested Asphalt Pavement.....	30
Figure 5-2 Variations of FN with Macrottexture MPD.....	32
Figure 5-3 Variations of FN with Microtexture MPD.....	33
Figure 5-4 Variations of FN with Microtexture SV and RMS.....	34

ACKNOWLEDGMENTS

This research project was sponsored by the Indiana Department of Transportation (INDOT) in cooperation with the Federal Highway Administration through the Joint Transportation Research Program (JTRP). The authors would like to thank Eliza Du of Indiana University-Purdue University Indianapolis (IUPUI) and Mark Leichty of Ames Engineering for their fruitful advices in the course of performing this study. Sincere thanks are extended to Becky McDaniel and Ayesha Shah of the North Central SuperPave® Center, and Kamron Yates of the INDOT their assistance in field friction and texture testing.

INTRODUCTION

Problem Statement

Over the past years, the Indiana Department of Transportation (INDOT) network pavement friction testing program has been continuously upgraded through research and the adoption of the state-of-the-art technologies so as to provide timely and reliable friction data for INDOT Districts and the Program Development Division to address pavement skidding safety issues and make more informed decisions on pavement maintenance and resurfacing. The INDOT annual pavement inventory friction testing is conducted in accordance with ASTM E 274 (1). ASTM E 274 utilizes a locked wheel trailer equipped with either ribbed or smooth test tires (2, 3). The standard test speed is 40 mph. However, safety concerns have been raised for the locked wheel friction testing method on high-speed highway facilities, particularly on interstate highways. This is primarily due to the nature of the locked wheel testing procedures. While conducting friction testing on high-speed facilities, the braking operation may impose significant impact on the traffic flow conditions.

In addition, the speed limit has been raised to 70 mph on most interstate highways in rural areas in Indiana. This further raises the safety concerns over the network pavement friction testing operation. Currently, the INDOT network pavement friction testing is conducted at a test speed of 30, 40 or 50 mph, depending on the real traffic conditions such as vehicle operating speed and traffic volume. The slow moving locked wheel trailer in the driving lane is a potential point of conflicts with high-speed vehicles. During the test season approximate between April and November each year, the network pavement inventory friction testing covers all interstate highways and one third of other roadways under INDOT's jurisdiction that add up to approximately 6,700 lane-miles. Therefore, it is a pressing need for INDOT to examine the potential safety issues associated with our network pavement friction inventory testing and explore new technologies for measuring pavement friction characteristics safely and efficiently at highway speeds.

Objectives

In an attempt to address the above concerns, this pilot study was initiated by the Joint Transportation Research Program (JTRP) to examine the so-called non-contact technologies, particularly the laser-based sensors, for quantitatively measuring pavement surface texture that has been considered as the sole variable affecting pavement surface friction characteristics. The laser-based sensors have been considered to be potentially well suited to measure the pavement surface texture continuously without having to be in contact with the pavement surface. The objectives were established for this pilot study. The first objective of the proposed pilot study is to assess the feasibility of using the laser-based sensor technology to measure pavement surface friction characteristics at highway speeds so as to make the INDOT network pavement friction testing program safer and provide a seamless coverage of the whole pavement network.

The second objective of this pilot study is to investigate the use of the laser-based sensor technology in measuring both macrotexture and microtexture measurements from a single test device. While macrotexture can be readily measured using laser-based sensors, no laser sensor has been reported to be capable of capturing microtexture at highway speeds to date. The microtexture is currently estimated as a surrogate using pavement friction at low speeds. However, the laser sensor technologies have advanced rapid to a point where high resolution, high accuracy laser sensors are commercially available. With this advancement has come the potential for measuring microtexture in the real-life pavements.

The third objective is to investigate the possible use of both macrotexture and microtexture in estimating pavement friction. Besides the safety concern associated with the friction testing using the locked wheel trailer on highway speed highway facilities, it is very difficult to measure pavement friction at the standard speed of 40 mph due to the real world traffic conditions. The conversion of friction numbers at other speeds to those at the standard speed requires the so-called speed gradients. However, speed gradients vary with pavement surface features and the type of test tire. It consumes much time and labor to establish speed gradients for the real world pavements based on both the ribbed and smooth tires. Pavement surface friction is a function of pavement surface texture characteristics. If both macrotexture and microtexture can be readily measured, it may become possible to evaluate pavement friction using texture measurements.

Scope of Work

In order to fulfill the objectives of the present study, the primary work will focus on the following areas:

- (1) Evaluation of the accuracy, repeatability and reproducibility of the sensor-based technology on the INDOT friction test track. While the test speed may have an effect on the texture measurement, it is reported that the technology works very well between 15 mph and 65 mph. This study will further address this issue.
- (2) Investigation of the technical requirements when selecting laser sensors for texture testing at highway speeds, which should be rigorous in theory, and sound in application.
- (3) Investigation of the measurements and calculation of the microtexture profile and characteristics.
- (4) Establishment of the inherent correlation between surface texture and friction characteristics by conducting testing on the friction test track.
- (5) Identify further needs for the use of laser-based sensors in estimating pavement friction from texture measurements.

CHARACTERISTICS OF PAVEMENT SURFACE TEXTURE AND FRICTION

Surface Texture Characteristics

In ASTM E 867 (4), pavement macrotexture is defined as the deviations of a pavement surface from a true planar surface with the characteristic dimensions of wavelength and amplitude from 0.5 mm up to those that no longer affect tire-pavement interaction, and pavement microtexture as the deviations of a pavement surface from a true planar surface with the characteristic dimensions of wavelength and amplitude less than 0.5 mm. The Permanent International Association of Road Congress (PIARC) conducted a study to investigate the effect of pavement surface texture on the tire-pavement interaction (5). In this PIARC study, pavement surface texture was characterized in terms of the texture wavelength and categorized into three groups below:

- (1) Microtexture: Wavelength < 0.02 in. (0.5 mm)
- (2) Macrotexture: Wavelength = 0.02 in. to 2 in. (0.5 mm to 50 mm)
- (3) Megatexture: Wavelength = 2 in. to 20 in. (50 mm to 500 mm)
- (4) Roughness: Wavelength > 20 in. (500 mm)

The peak-to-peak amplitude varies between 0.01 and 50 mm for the macrotexture, and between 0.001 and 0.5 mm for the microtexture. The PIARC study further investigated the effects of the surface texture characteristics on the correlation between texture wavelength and on the tire-pavement interaction including wet friction, noise, splash and spray, rolling resistance, and tire wear as shown in Figure 2-1. It was concluded that both microtexture and macrotexture ultimately determine the wet-pavement friction. Kummer indicated that fundamentally, the friction force consists of adhesion force and hysteresis force (6). The former depends mainly on the microtexture and the latter on the macrotexture. In addition, the macrotexture affects the surface drainage and therefore the water splash and spray.

As microtexture and macrotexture increase, pavement surface friction increases. However, an attempt to enhance pavement friction by increasing surface texture may result in high noise, splash and spray, and tire wear problems. Therefore, the design of surface texture requires a compromise among friction, noise, splash and spray, and tire wear. However, texture is the physical property of pavement surface, which does not change regardless of the surrounding environment condition and regardless of the type of test equipment. There is no doubt that if pavement surface texture can be quantitatively determined, it can be readily translated into the conventional friction measurement, such as the so-called friction or skid number.

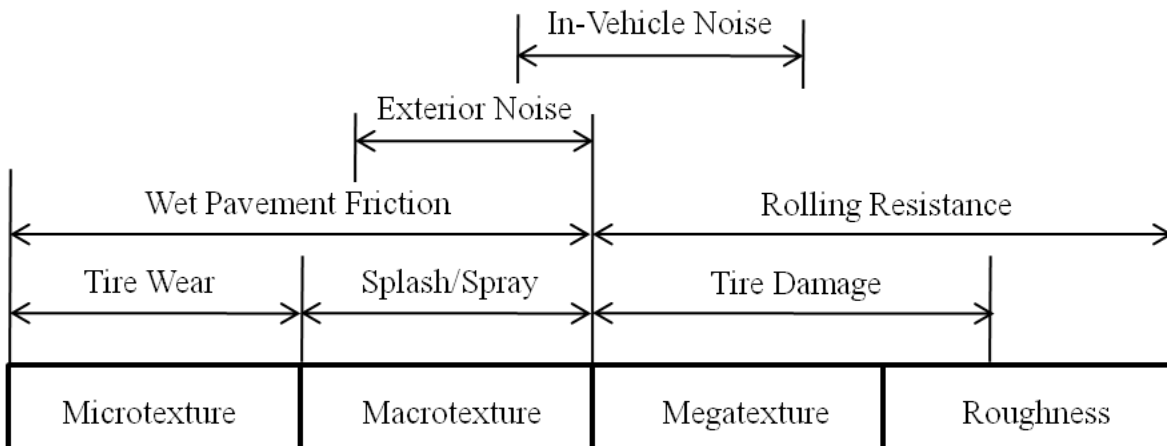


Figure 2-1 Texture Wavelengths and Impacts

(Source: PIARC [5])

Henry investigated the relationship between surface texture and friction force (7). When water is presented at the tire-pavement interface, bulk water is first removed through macrotexture, and then, the water film between tire and pavement surface is wiped out in part by the leading edge of tire tread. Therefore, the adhesion force diminishes. However, the hysteresis force is little sensitive to water. Consequently, the friction force decreases on wet pavement due to the decrease in adhesion force. When pavement surface is smooth and dry, the friction force is dominated by the adhesion force. Henry also indicated that the ribbed tire was not sensitive to pavement surface macrotexture but are dominated by the microtexture because the grooves on the ribbed tire provide channels much larger than the macrotexture for water flow.

Quantitative Texture Measurements

The Mean Profile Depth

The so-called mean profile depth (MPD) is adopted by ASTM E 1845 (8) to quantitatively characterize the macrotexture. The MPD has been shown to be useful in predicting wet pavement friction and is calculated from a profile of pavement macrotexture with a baseline length of 100 mm that is two times as large as the maximum wavelength of the macrotexture. As illustrated in Figure 2-2 is a macrotexture profile of 100 mm. The calculation process of MPD consists of three main steps, including calculation of a linear equation of $Y=a+bX$, calculation of Peak1 and Peak2, and calculation of the average value of Peak1 and Peak2 as follows (5, 8):

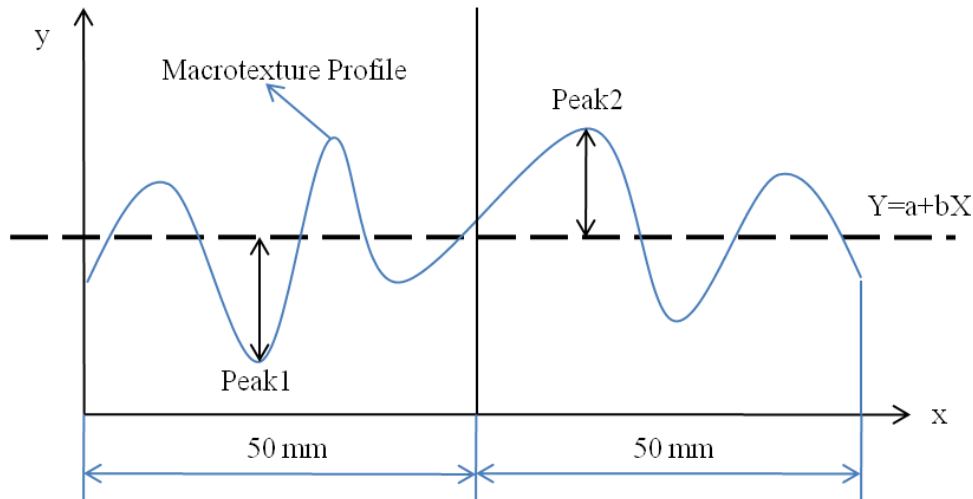


Figure 2-2 Illustration of Texture Computation

(1) Calculation of $y=a+bx$. In reality, the linear equation of $Y=a+bX$ determines the average level of the 100-mm long segment of macrotexture profile. In $Y=a+bX$, “a” is the intercept and “b” is the slope. The calculation of a and b is described below:

- Divide the 100-mm segment into n equal parts, and then the evenly spaced points, i.e. x_0, x_1, x_2, \dots and x_n (n is an even number) can be determined. Determine the y-coordinates of the macrotexture profile with respect to x_0, x_1, x_2, \dots and x_n , i.e. y_0, y_1, y_2, \dots and y_n .
- Perform linear analysis to determine a and b as follows (9):

$$\text{Slope: } b = \frac{SS_{xy}}{SS_{xx}} \dots\dots\dots(2-1)$$

$$\text{Intercept: } a = m_y - bm_x \dots\dots\dots(2-2)$$

$$\text{Coefficient of Correlation: } r^2 = \frac{SS_{xy}^2}{SS_{xx} SS_{yy}} \dots\dots\dots(2-3)$$

where m_x , m_y , SS_{xx} , and SS_{xy} are calculated as follows:

$$m_x = \frac{\sum x_i}{n} \dots\dots\dots(2-4)$$

$$m_y = \frac{\sum y_i}{n} \dots\dots\dots(2-5)$$

$$SS_{xx} = S_{xx} - n m_x^2 \dots\dots\dots(2-6)$$

$$SS_{yy} = S_{yy} - n m_y^2 \dots\dots\dots(2-7)$$

$$SS_{xy} = S_{xy} - n m_x m_y \dots\dots\dots(2-8)$$

$$S_{xx} = \sum x_i^2 \dots\dots\dots(2-9)$$

$$S_{yy} = \sum y_i^2 \dots\dots\dots(2-10)$$

$$S_{xy} = \sum x_i y_i \dots\dots\dots(2-11)$$

$$SS_{xx} = S_{xx} - n m_x^2 \dots\dots\dots(2-12)$$

$$SS_{yy} = S_{yy} - n m_y^2 \dots\dots\dots(2-13)$$

$$SS_{xy} = S_{xy} - n m_x m_y \dots\dots\dots(2-14)$$

(2) Determine the two Peaks, i.e. Peak1 and Peak2 as follows:

- In the first half 50-mm segment

$$\text{Compute: } \Delta y_{1_i} = |y_i - Y_i| \quad (i = 1, 2, \dots, n/2) \dots\dots\dots(2-15)$$

$$\text{Peak1} = \text{Max} \{ \Delta y_{1_i} \} \dots\dots\dots(2-16)$$

where y_i and Y_i are the measured y-coordinate and predicted y-coordinate with respect to x_i , respectively.

- In the second half 50-mm segment

$$\text{Compute: } \Delta y_{2_i} = |y_i - Y_i| \quad (i = n/2, (n+1)/2, \dots, n) \dots\dots\dots(2-17)$$

$$\text{Peak2} = \text{Max}\{ \Delta y_{2_i} \} \dots\dots\dots(2-18)$$

where y_i and Y_i are as defined earlier.

- (3) Compute the mean of Peak1 and Peak2, i.e. the so-called mean segment depth (MSD) for the 100-mm segment

$$MSD = \frac{\text{Peak1} + \text{Peak2}}{2} \dots\dots\dots(2-19)$$

For a pavement section longer than 100 mm, it is needed to divide the entire pavement section into 100-mm long segments. After MSD is determined for each segment, the MPD for the entire pavement section is the mean value of MSD values for all segments.

Other Measurements

In addition to the MPD, there are two supplemental variables that may be useful for quantifying surface texture characteristics. The first is slope variance, i.e., SV that measures the sharpness of pavement surface asperities (10). Surface asperities mainly affect the hysteresis component of the friction force. It is believed that it is possible to achieve a good correlation between the macrotexture and friction measurements by taking into account the slope variance in addition to the mean profile depth. The slope variance can be calculated as follows:

- (1) Divide the test section into various 100-mm segments ($j = 1, 2, \dots, N$)
- (2) Read coordinates of the macrotexture profile for each 100-mm segment:
x-coordinates: $x_0, x_1, x_2, \dots, x_n$, and y-coordinates: $y_0, y_1, y_2, \dots, y_n$
- (3) Calculate individual slopes, i.e., SV_1, SV_2, \dots, SV_n for the 100-mm segment as follows:

$$SV_i = \frac{y_{i+1} - y_i}{x_{i+1} - x_i} = \frac{\Delta y_i}{\Delta x_i} \quad (i=0, 1, 2, \dots, n-1) \dots \dots \dots (2-20)$$

(4) Calculate the root mean square of all SV_i values as follows:

$$SV = \sqrt{\frac{\sum SV_i^2}{n}} \quad (i=0, 1, 2, \dots, n-1) \dots \dots \dots (2-21)$$

where SV is defined as the slope variance.

The second supplemental variable is the root mean square (RMS) of the macrotexture profile. RMS is a measure of the magnitude of the asperities of a macrotexture profile through erasing the signs of the negative peak values. The calculation procedures of RMS are as follows:

- (1) Divide the test section into various 100-mm segments ($j = 1, 2, \dots, N$)
- (2) Read coordinates of the macrotexture profile for each 100-mm segment:
x-coordinates: $x_0, x_1, x_2, \dots, x_n$, and y-coordinates: $y_0, y_1, y_2, \dots, y_n$
- (3) Perform linear regression (see the calculation of MPD)
- (4) Perform calculations below:

$$\Delta y_i = |y_i - Y_i| \quad Peak_i = |y_i - Y_i| \quad (i=1, 2, \dots, n) \dots \dots \dots (2-22)$$

(5) Calculate the RMS

$$RMS = \sqrt{\frac{\sum Peak_i^2}{n}} \quad (i=1, 2, \dots, n) \dots \dots \dots (2-23)$$

Since there is no standard practice and method for microtexture testing and quantitative characterization, the measures similar to those for characterizing the macrotexture, such as the mean profile depth, slope variance, and root mean square, were utilized to characterize the pavement surface microtexture. This will be discussed in detail in Chapter 3.

TEXTURE LASER SYSTEMS AND TEST SETUP

Selection of Texture Laser Measuring Systems

Frequency of Pavement Texture Wave

The selection of the laser measuring system depends not only on the texture waveband and amplitude, but also on the frequency of the texture. In the fundamental physics (11), frequency is defined as the number of a repeating or periodic event, such as oscillations, vibrations, or waves occurring per unit of time. In general, the frequency is related to the wavelength and velocity as follows:

$$f = \frac{v}{\lambda} \dots\dots\dots(3-1)$$

where v is the so-called phase velocity; λ is the wavelength; and f is the frequency. The frequency defined in Eq. (3-1) is also referred to as temporal frequency with a unit of hertz (Hz), and its reciprocal is called the period.

It is indicated that in Chapter 2, the pavement texture is currently characterized by the wavelength and amplitude. For pavement macrotexture, the wavelength and amplitude vary from 0.5 mm to 50 mm. For pavement microtexture, the wavelength and amplitude are less than 0.5 mm. However, the frequency and velocity have not been identified in pavement texture due probably to the fact that in nature, pavement texture is physical, static object. In reality, the laser system is usually mounted on a test vehicle. During the field pavement texture testing, the test vehicle travels on the pavement at a certain speed. This indicates that the laser mounted on the test vehicle scans the pavement surface at the same speed as the vehicle. In other words, the pavement texture can be considered as a wave passing the laser at the speed of test vehicle. Therefore, replacing the velocity in Eq. (3-1) with the speed of test vehicle gives the frequency of pavement texture with a certain wavelength as shown in Table 3-1.

Table 3-1 Pavement Texture Frequencies by Wavelength at Different Speeds

Test Vehicle Speed (mph)	Frequency by Wavelength (Hz)			
	50-mm	0.5-mm	0.03-mm	0.001-mm
10	89	8939	148981	4469444
20	179	17878	297963	8938889
30	268	26817	446944	13408333
40	358	35756	595926	17877778
50	447	44694	744907	22347222
60	536	53633	893889	26816667

Requirements for Texture Laser Systems

In order to capture accurate and reliable information on the characteristics of both macrotexture and microtexture, the laser should meet the necessary requirements for laser spot size, sampling resolution, sampling spacing, and sampling frequency. For macrotexture, the requirements given in ASTM E 1845 are as follows:

- Laser spot size: No greater than 1 mm
- Vertical resolution: 0.05 mm or better
- Sampling spacing: No more than 1 mm

The sampling frequency is another important indicator of the texture measuring capability of the laser. One published study indicates that the laser sampling frequency should be great enough to handle the signal variations caused by the background fluctuations (12). Some researchers indicated that the sampling frequency of the laser should meet the requirement by the Nyquist sampling theorem (13). Fundamentally, the Nyquist sampling theorem forms the requirement of the nominal sampling interval to avoid aliasing (14), and states that the sampling frequency should be at least twice the highest frequency contained in the signal. Note that the real world pavement texture is usually complex and consists of many wavelength components that produce different frequencies. The laser’s sampling frequency should be at least twice the highest frequency according to the Nyquist sampling theorem.

As an example, pavement macrotexture has a wavelength of 0.5 mm to 50 mm. The highest frequency arrives with respect to the wavelength of 0.5 mm. Therefore, the required sampling frequency for a laser system can be determined according to the traveling speed of the

test vehicle as shown in Figure 3-1. It is shown that theoretically, a laser with a sampling frequency of 54 kHz is capable of capturing all peaks and troughs of the pavement macrotexture at 30 mph. At 50 mph, the required sampling frequency may be up to 90 kHz. After weighing the study goal, the accuracy requirement, and the potential safety issues, two types of lasers were selected by this study, including a 1 kHz laser scanner, and a 62.4 kHz laser system. The 1 kHz laser scanner is a stand-alone system (see Figure 3-2) and the 62.5 kHz laser system is a pointer laser mounted on a test vehicle as shown in Figure 3-3.

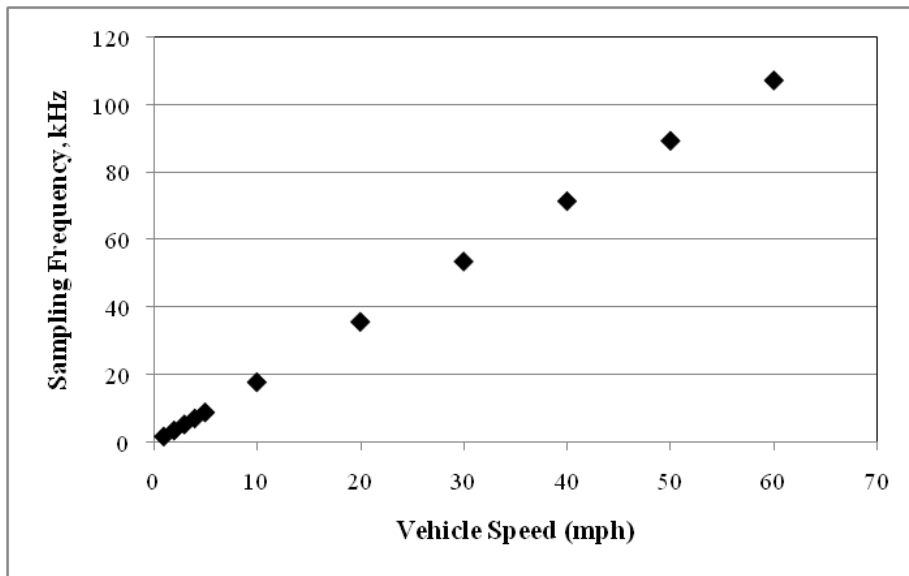


Figure 3-1 Laser’s Sampling Frequency Required at Different Test Speeds



Figure 3-2 The 1 kHz Laser Texture Scanner



Figure 3-3 The 62.5 kHz Laser System Mounted on a Test Vehicle

Table 3-2 shows the specifications for these two laser systems (15, 16). Also presented in Table 3-2 are the specifications for the laser of the circular track meter (CTMeter) in ASTM E 2157-09 (17). Since the 1 kHz laser scanner has a very low scanning speed (approximately 15 mm/sec), high resolution, and small spacing, it was utilized to provide microtexture measurement references, and to better understand the characteristics microtexture. The 62.4 kHz laser system has a variable sampling spacing that depends on the speed and is capable of capturing all macrotextures and some microtextures at relatively high speeds. A published study has confirmed that such a laser can produce a repeatable and accurate measure of macrotexture at variable speeds (18), and however, issues arose on tined (or grooved) concrete pavement. It was also believed that the 62.4 kHz laser is capable of capturing some microtexture (19). Therefore, the 62.5 kHz laser was utilized to further address these issues.

Table 3-2 Laser System Specifications

Description	1-kHz Laser	62.4-kHz Laser	CTMeter
Laser spot size	0.050 mm	0.55 mm	0.07 mm
Vertical Resolution	0.015 mm	0.031 mm	0.003 mm
Sampling Spacing	0.015 mm	~	0.87 mm
Wavelength Range	0.03 mm to 50 mm	All macro- and part of microtexture	Not Available

Pavement Texture Testing

The INDOT Friction Test Track

Pavement texture Profile data was first collected on the INDOT friction test track that consists of three different pavements, such as slick concrete pavement, hot mix asphalt (HMA) pavement, and tined concrete pavement (see Figure 3-4). The three surfaces were specially prepared to represent the possible magnitude of pavement surface friction on the real world highways. The HMA pavement was constructed with 9.5-mm SuperPave© mix. Both the slick and tined concrete pavements were constructed with regular cement concrete mix. However, the slick concrete pavement was finished to provide a smooth surface that is usually observed on highways experiencing very poor friction. The tined concrete surface was finished with 3-mm deep, 3-mm wide transverse grooves at a spacing of 18-20 mm. Summarized in Table 3-2 are the surface friction properties of these three pavements.



Figure 3-4 INDOT Friction Test Track

Table 3-3 Friction Properties of the Friction Test Track Surfaces

Pavement Surface	Dynamic Friction Tester (9)			Locked Wheel FN at 40 mph
	MPD (mm)	DFT	IFI	
Slick Concrete	0.08	0.374	0.123	8.8
9.5-mm HMA	0.59	0.671	0.352	42.5
Tined Concrete	1.45	0816	0.534	59.0

Possible Effect of Sunlight

As an experimental testing, this study measured the macrotexture data on the slick concrete surface using the 1 kHz laser system on a sunny day. Figure 3-5 shows the results of MPD and RMS measured at different time throughout the day. MPD and RMS varied dramatically over time. Both the MPD and RMS increased after the start, peaked at 11:20am, and decreased after 11:20am. This study further measured the macrotexture data on the tined concrete surface in two scenarios, respectively, and the results are presented in Table 3-3. In Scenario I, the laser system was covered with a carton box to shed the sunlight while testing. In Scenario II, the laser system was not covered in a carton box. All the three tests generated almost the same results in Scenario I. In Scenario II, both MPD and RMS increased dramatically. A possible explanation is that the laser system was not setup appropriately and could not filter out the spectrum of sunlight (20). The above observation is the first of its type ever reported. In order to eliminate the possible effect of sunlight, the 1 kHz laser system was always covered with a carton box during testing. No effect was observed on the 62.4 kHz laser system.

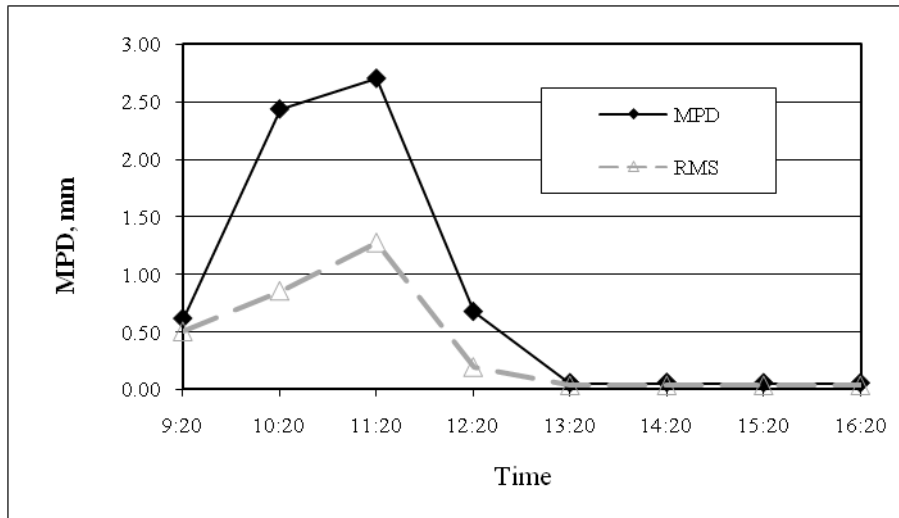


Figure 3-5 MPD Values Measured at Different Time

Table 3-4 Comparison of MPD on Tined Concrete Surface

Test Run	MPD, mm	RMS, mm	Test Scenario
Run 1	1.487	1.115	Scenario 1
Run 2	1.487	1.115	Scenario 1
Run 3	1.488	1.116	Scenario 1
Run 4	3.466	1.723	Scenario 2

Possible Effect of Test Speed

The 62.5 kHz laser system served because of two reasons. First, a published study has confirmed that such a laser can produce a repeatable and accurate measure of macrotexture MPD at variable highway speeds. Second, it was believed that the 62.4 kHz laser is capable of capturing part of the microtexture at highway speeds. This study also measured the macrotexture data on the INDOT friction test track using the 62.5 kHz laser at 40 km/h (25 mph) and 48 km/h (30 mph), respectively. The calculated macrotexture variables, such as MPD, SV, and RMS, are presented in Table 3-4. It is shown that the variables are very close at two different speeds, regardless of the type of pavement surface. Although there are some minor differences, this is probably due to the fact that it is hard to measure the same texture profile in the field testing. Again, it is confirmed that a 62.5 kHz laser is capable of producing a repeatable and accurate measure of macrotexture profile at different speeds. This can be extended to conclude that a longitudinal profile of macrotexture produced using a 62.5 kHz laser not only has unique MPD, but also has unique SV and RMS, regardless of the test speed.

Table 3-5 Measurements of Macrotexture at Different Speeds

Texture Variables	Speed (km/h)	Slick Surface	HMA Surface	Tined Concrete
MPD (mm)	40	0.615	0.975	1.611
	48	0.611	1.067	1.579
SV	40	0.971	1.085	1.506
	48	0.912	0.961	1.462
RMS (mm)	40	0.310	0.448	1.051
	48	0.315	0.498	1.100

TEXTURE DATA ANALYSIS

Surface Macrotexture

Macrotexture Profiles

As mentioned in Chapter 3, the 1 kHz laser scanner was setup for a sampling spacing of 0.015 mm at a scanning rate of approximately 15 mm/sec. In order to capture the properties of the macrotexture profile with a texture wavelength of 0.50 mm to 50 mm and reduce the potential effect of the noise and transients, the raw texture profiles measured by the 62.5 kHz point laser were filtered and converted into macrotexture profiles with a highpass cutoff of 50 mm and a lowpass cutoff of 0.5 mm. The sampling spacing was adjusted to 0.1702 mm, i.e., one third of the lowpass cutoff. Theoretically, the 1 kHz laser scanner can better capture the spatial variations in the texture profile than the 62.5 kHz point laser, simply because the 1 kHz laser's sampling spacing is much smaller than the 62.5 kHz laser's sampling spacing. This study measured pavement macrotexture profiles using both the 1 kHz and 62.6 kHz lasers on the INDOT friction test track as plotted in Figure 4-1.

As pointed out that in Chapter 3, it was very hard to measure the same profile since the 62.5 kHz laser was mounted on a test vehicle. It is natural that the two macrotexture profiles display variations with different patterns. However, it looks that the two macrotexture profiles vary in the same range in terms of the magnitude of the spikes and the magnitude of the troughs on the HMA surface. On the tined concrete surface, it appears that the spikes detected by the two lasers have the same magnitude. The two lasers were also capable of detecting all grooves that have a spacing of approximately 20 mm. While the groove depth detected by the 1 kHz laser is noticeably greater than that by the 62.5 kHz laser, the groove depths detected by the two lasers are still in the same order of magnitude. On the slick concrete surface, however, the spikes and troughs detected by 1 kHz and 62.5 kHz lasers are completely in different order of magnitude. The 1 kHz laser scanner tended to produce spikes and troughs that are less than those by the 62.5 kHz laser.

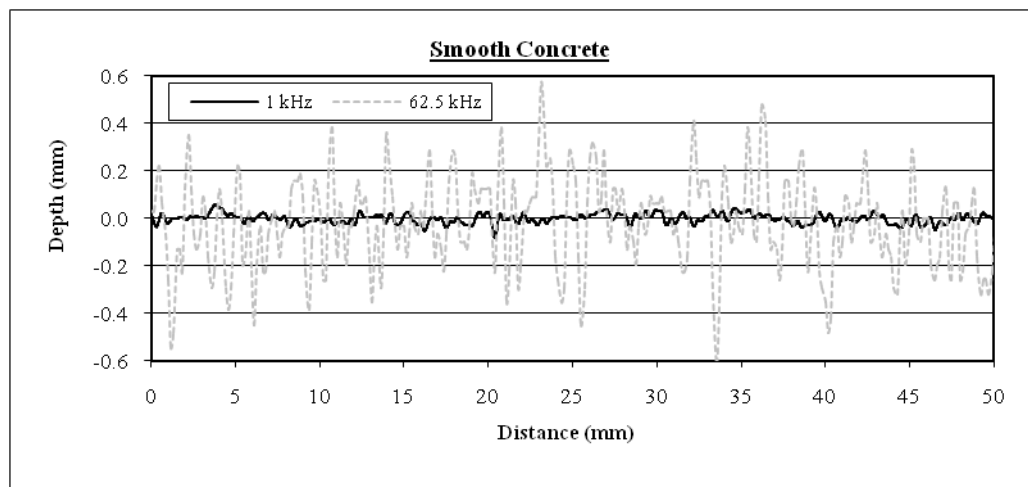
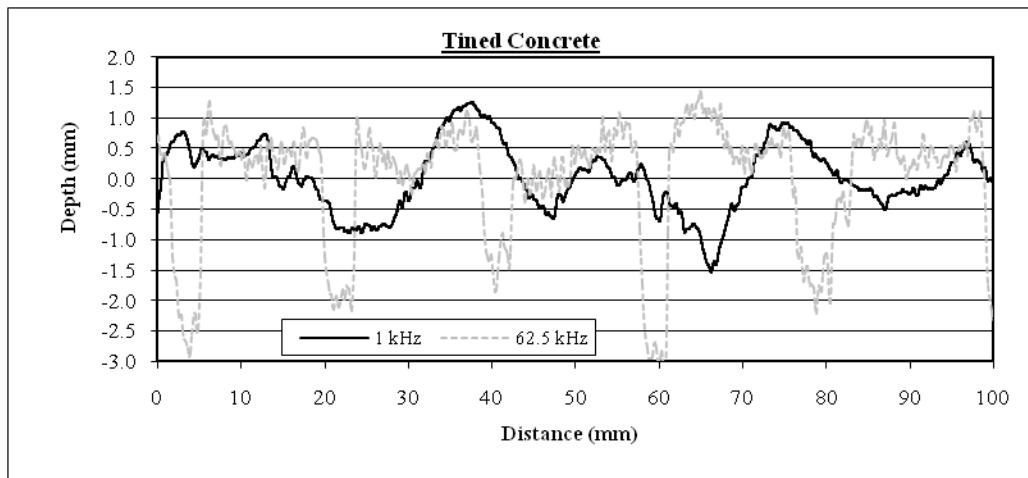
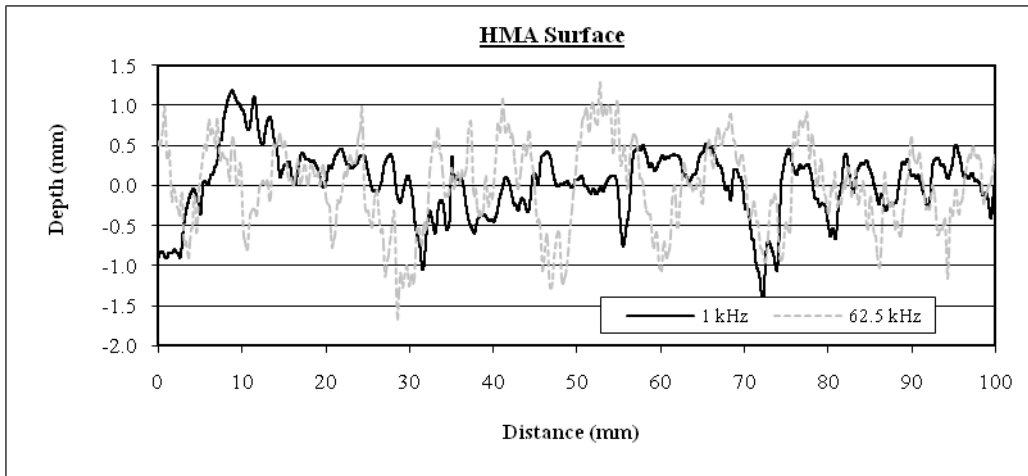


Figure 4-1 Typical Macrotexture Profiles Measured Using 1 kHz and 62.5 kHz Lasers

Mean Profile Depth

Table 4-1 shows the MPD values measured by three lasers, including the 1 kHz laser scanner, the 62.5 kHz point laser and the CTMeter, respectively. The CTMeter consists of a charge coupled laser that is mounted on an arm that rotates so that the laser follows a circular track having a diameter of 284 mm. It is shown that the macrotexture depths are in different magnitudes on the three surfaces. It is also shown that on the tined concrete surface, the MPD values measured by the three devices show very good agreement. On the 9.5-mm HMA surface, the MPD values measured by the 1 kHz laser and 62.5 kHz laser show good agreement and are almost twice the MPD measured by the CTMeter. On the slick concrete surface, the MPD measured by the 62.5 kHz laser is approximately 14 times the MPD measured by the 1 kHz laser, and 9 times the MPD measured by the CTMeter. The MPD values measured by the 1 kHz laser and the CTMeter display noticeable difference, but are in the same order of magnitude.

Table 4-1 Summary of MPDs Measured by Different Devices

Pavement Type	MPD by Different Devices (mm)		
	1 kHz Laser	62.5 kHz Laser	CTMeter
Slick concrete	0.051	0.694	0.08
9.5-mm HMA	1.156	1.020	0.59
Tined Concrete	1.487	1.479	1.45

It can be simply concluded that the 62.4 kHz laser is capable of producing reliable properties of the macrotexture profiles on the tined concrete pavements. On the 9.5-mm HMA pavement, the 62.5 kHz laser is capable of producing the properties of macrotexture profiles in good agreement with those by the 1 kHz laser. Notice that the CTMeter laser has a tangent speed of 6 m/s and a sampling rate of 1024 times/revolution. In other words, the sampling frequency of the CTMeter is 115 Hz. Also, while the CTMeter's vertical resolution is 0.003 mm, this resolution may not be achievable since the CTMeter's laser spot size (see Table 3-2) is much greater than the vertical resolution. However, it may indicate that the 62.5 kHz laser is probably not capable of producing accurate macrotexture profiles on very slick pavements. One possible reason is that on very slick surfaces, the macrotexture profile consists mainly of texture components having very small wavelengths and amplitudes that the 62.5 kHz laser is unable to capture.

Surface Microtexture

Microtexture Profiles

As plotted in Figure 4-2 are the microtexture profiles measured on the three pavement surfaces such as the slick concrete, HMA, and tined concrete surfaces using the 1 kHz laser scanner and the 62.5 kHz point laser, respectively. Apparently, the two microtexture profiles are significantly different from each other and display different variations. The 62.5 kHz laser tended to produce a microtexture profile with spikes and troughs that are much greater than those of the microtexture profile measured by the 1 kHz laser. This is similar to the observation made on the macrotexture measurements on the slick concrete surface. One possible reason is that the 62.5 kHz laser might not be capable of capturing those microtextures having very short wavelengths and very small amplitudes (spikes and troughs). Consequently, the so-called “aliasing” might arise, which could not only cause the loss of important information about the characteristics of the microtexture, but also produce wrong information about the properties of the microtexture.

To minimize the possible problem of “aliasing”, all the microtexture data used in the analysis of microtexture was collected using the 1 kHz laser scanner. Figure 4-3 shows the typical microtexture profiles measured using the 1 kHz laser on the slick concrete, HMA and tined concrete surfaces, respectively. An interesting observation is that the variations of microtexture depths are in a similar range regardless of the type of surface. This is different from the observation on the macrotexture profiles (see Figure 4-1), which indicates that the macrotexture depths varied on different magnitude levels. Figure 4-4 shows the microtexture profiles for a 1-mm long segment extracted from the three microtexture profiles using the 1 kHz laser in Figure 4-3. Two observations can be made through careful inspection of these three microtexture profiles. First, the microtexture profile consists of many wavelength (or frequency) components. It should be reiterated that since the 1 kHz laser has a profile wavelength range of 0.03 mm to 0.5 mm, the highest frequency arises with respect to the wavelength of 0.03 mm. Second, the microtexture profile on the HMA surface demonstrated great variations. The hypothesis is that in the HMA mix, the coarse aggregates consisted of not only crushed stone, but also 27% of steel slag and 27% of dolomite. The steel slag and dolomite aggregates are highly angular in shape and provide rough texture.

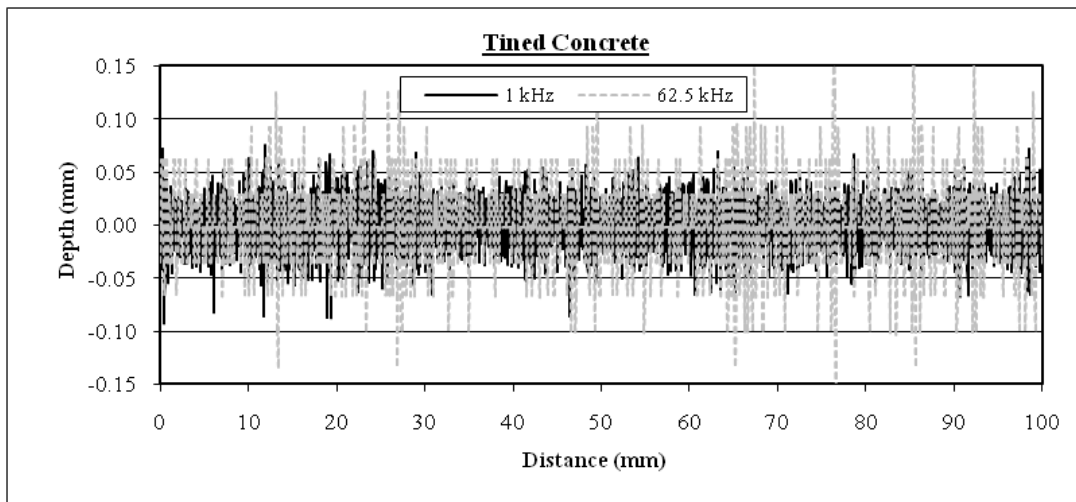
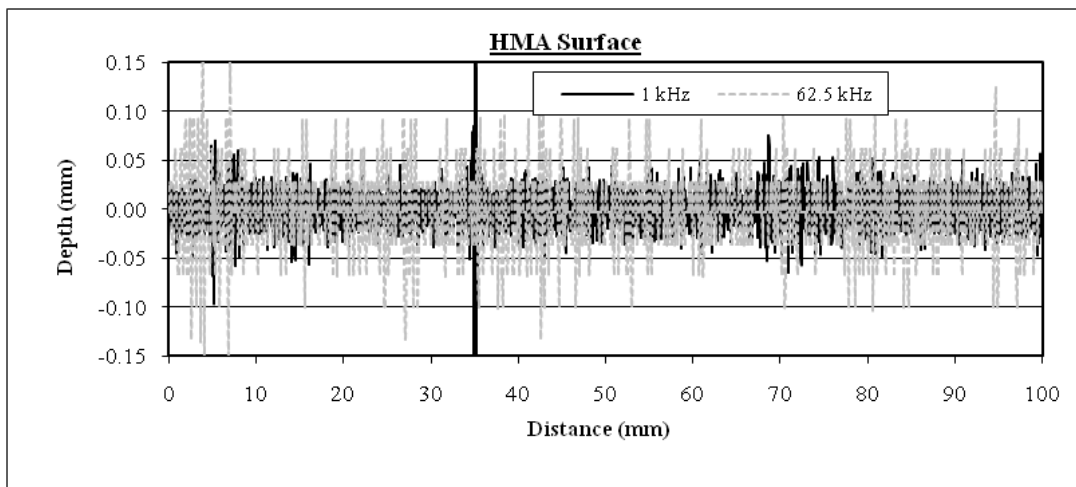
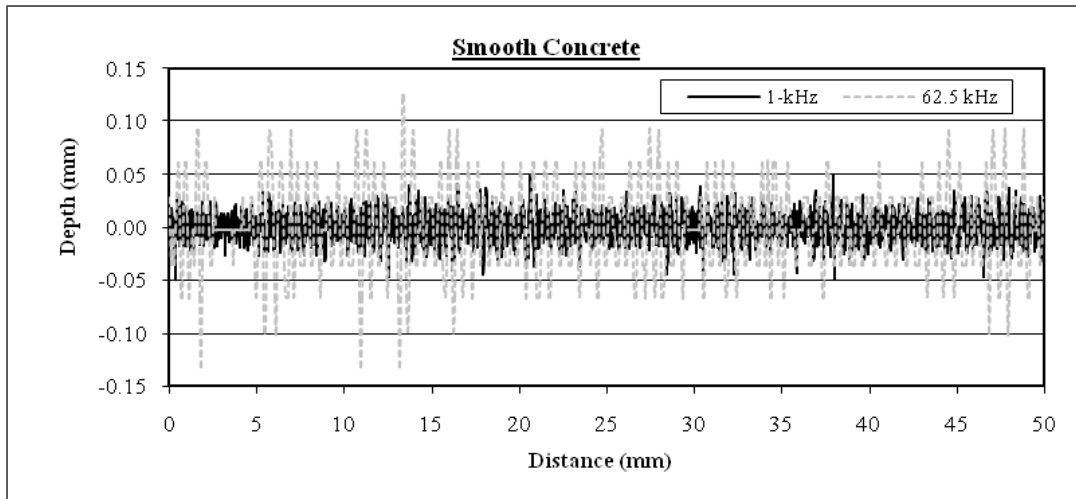


Figure 4-2 Microtexture Profiles Measured on Three Surfaces

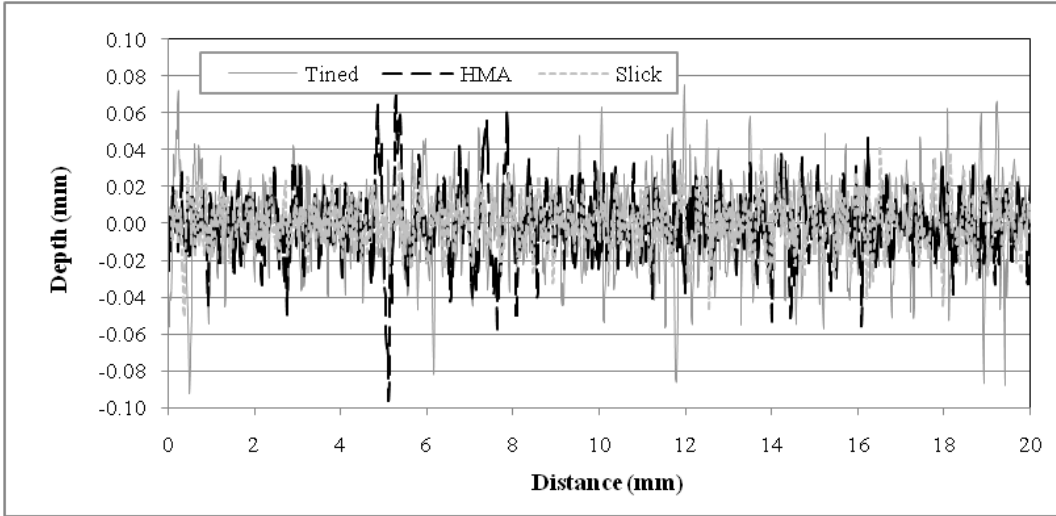


Figure 4-3 Typical Microtexture Profiles on Three Surfaces

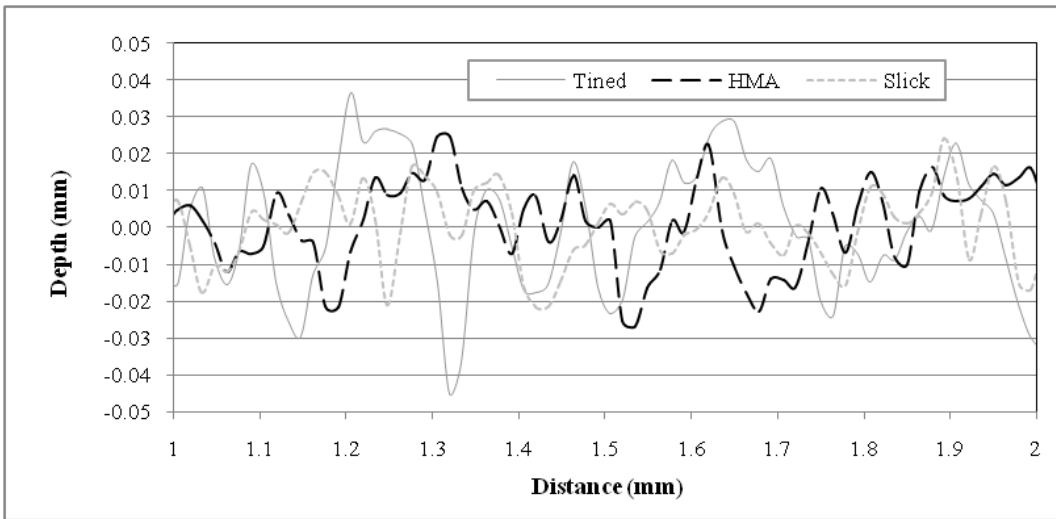


Figure 4-4 Microtexture Profiles on a 1-mm Long Segment Surface

Microtexture Depth and Wavelength

Figure 4-5 shows the distributions of texture depths for the microtexture profiles measured on the slick concrete, HMA, and tined concrete surfaces, respectively. The vertical axis, i.e., the accumulated distribution, indicates the total percentage of the texture depths less than a certain value or simply the percentile. It is shown that the texture depth usually is less than 0.05 mm. Summarized in Table 4-2 is the information on the distributions of microtexture depths, including the average texture depth, the standard deviation (Stdev), and the coefficient of variation for these three pavement surfaces, respectively. Also tabulated in Table 4-2 are the

texture depths for different percentiles. Apparently, the tined concrete surface exhibits the greatest texture depth, and the slick concrete surface exhibits the smallest texture depth. However, the slick and tined concrete surfaces demonstrate the similar degree of variations (see the COV values), and the HMA surface demonstrates the greatest variability due probably to the use of steel slag and dolomite aggregates.

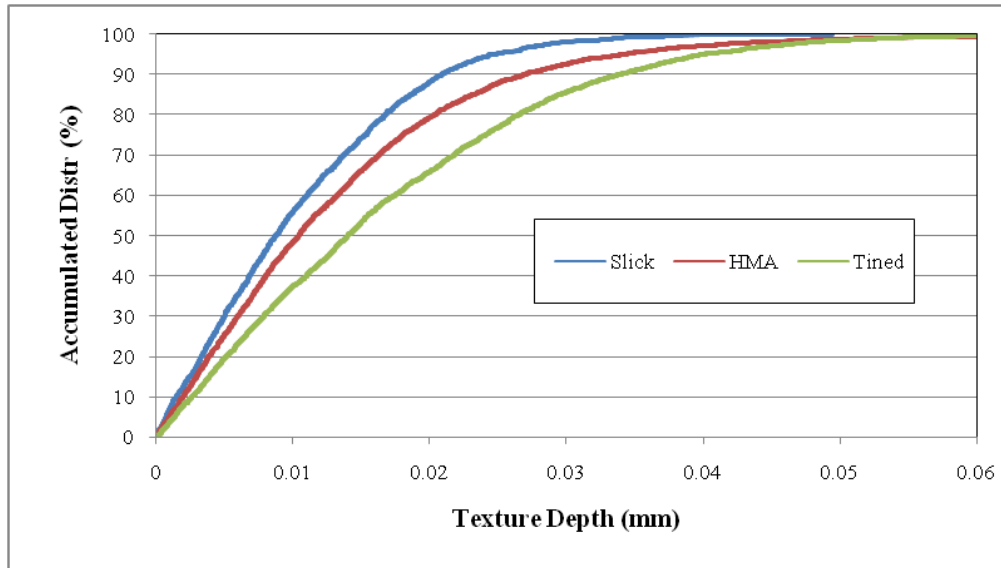


Figure 4-5 Distributions of Microtexture Depths on Three Surfaces

Table 4-2 Summary of the Distributions of Microtexture Depth

Percentile	Slick Concrete	HMA	Tined Concrete
50 th	0.009	0.010	0.014
70 th	0.014	0.016	0.022
85 th	0.019	0.023	0.030
90 th	0.021	0.027	0.034
95 th	0.025	0.034	0.040
100 th	0.049	0.050	0.075
Ave Depth (mm)	0.010	0.014	0.017
Stdev. (mm)	0.008	0.021	0.013
COV	75.5	148.7	75.9

In order to examine the variations of microtexture wavelength, this study manually measured the wavelength of microtexture from the plot of 1-mm long microtexture profile as shown in Figures 4-6. For each type of surface, ten 1-mm long segments were measured. The wavelengths were computed in two different approaches. Careful inspection of Figure 4-6

indicates that the microtexture profile is composed of two categories of waves, i.e., large-scale and small-scale waves. The large-scale wave indicates the overall shape of the profile (see the broken line in Figure 4-6), and the small-scale wave indicates the local roughness of the profile line, i.e., the deviations from the large-scale wave. The wavelengths were computed by counting the number of both spikes and troughs over a certain distance.

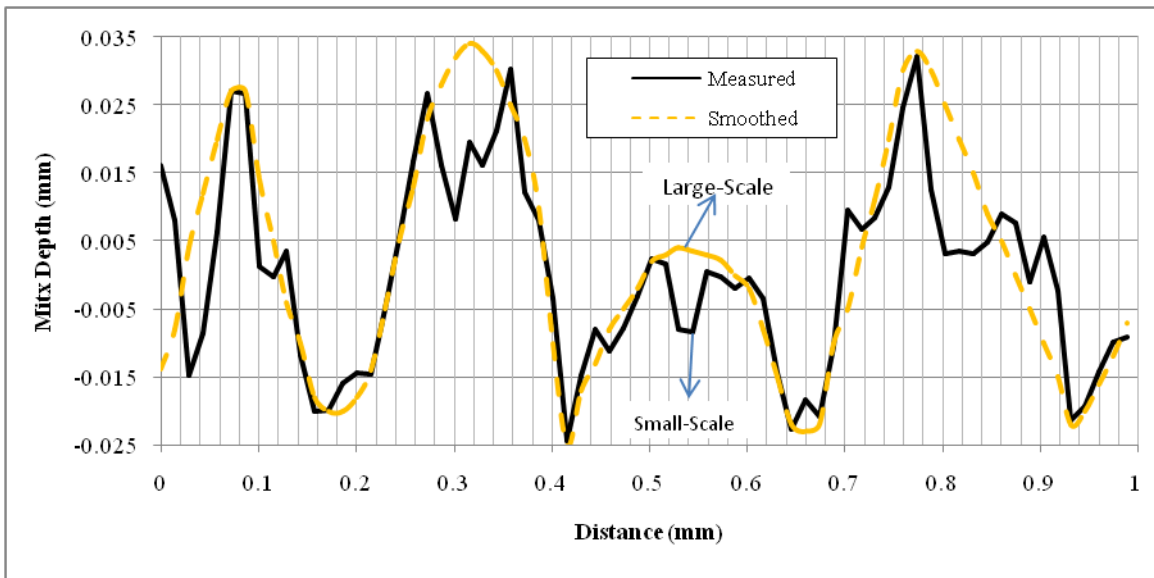


Figure 4-6 Example Plot for Manual Calculation of Wavelength

Table 4-3 shows the results of the wavelengths computed for these three pavement surfaces, respectively. For the large-scale waves, the largest wavelength is 0.475 mm on the tined concrete surface, 0.395 on the slick concrete surface, and 0.290 on the HMA surface. However, the average wavelength on the HMA surface is 0.170 mm that is greater than those on both the slick and tined concrete surfaces. This is because the microtexture wavelength distributions on these two concrete surfaces are extremely right-skewed over a large range and have relatively few large wavelength values, in particular on the tined concrete surface (see Figure 4-7). Nevertheless, the distribution of microtexture wavelength on the HMA surface is relatively flat over a small range. For the small-scale waves, the wavelengths are almost the same for the three surfaces in terms of the average wavelength, standard deviation, or distribution range. Therefore, the differences between the microtexture profiles of the three pavement surfaces are mainly associated with the large-scale waves.

Table 4-3 Summary of Microtexture Wavelength Statistics

Wavelength Statistics	Slick Concrete		HMA		Tined Concrete	
	Small-Scale	Large-Scale	Small-Scale	Large-Scale	Small-Scale	Large-Scale
Ave (mm)	0.046	0.131	0.046	0.172	0.043	0.151
Stdev (mm)	0.013	0.062	0.013	0.054	0.013	0.073
COV (%)	28.3	47.3	28.3	31.4	30.2	48.3
N	90	67	110	45	102	52
Max (mm)	0.085	0.395	0.080	0.290	0.080	0.475
Min (mm)	0.025	0.050	0.020	0.075	0.020	0.070

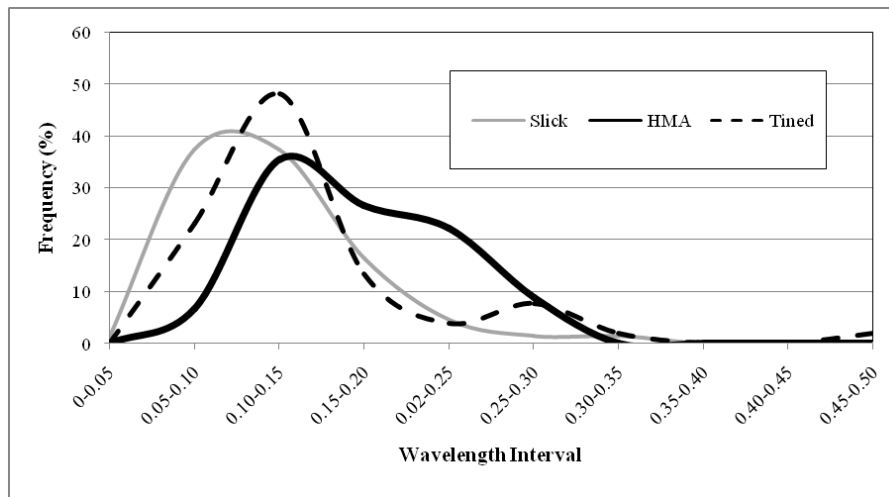


Figure 4-7 Microtexture Wavelength Distributions on Three Surfaces

Measurement of Microtexture Properties

Determination of Microtexture Baseline Length

Currently, there is no standard or specification available for measuring the properties of pavement surface microtexture. Since both microtexture and macrotexture are pavement surface textures, the procedures for calculating the MPD of a macrotexture profile were adopted by this study to analyze the microtexture data. Notice that in the calculation of the MPD of a macrotexture profile, there are two important variables, including the baseline length and the texture depth. It is well-known that the baseline length for calculating the MPD of a macrotexture profile is 100 mm that is exactly twice the maximum wavelength of macrotexture. Basically, the MPD is the average of the two peak depths, one in each of the two 50-mm segments. This study

computed the microtexture MPD, SV, and RMS based on various baseline lengths, which are presented in Figure 4-8.

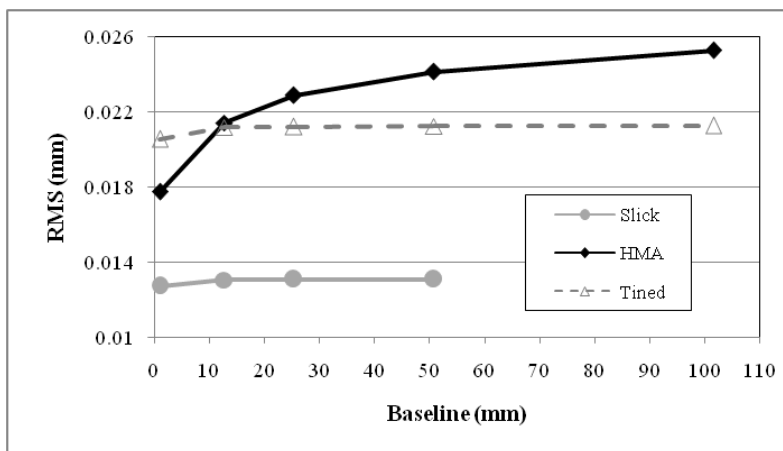
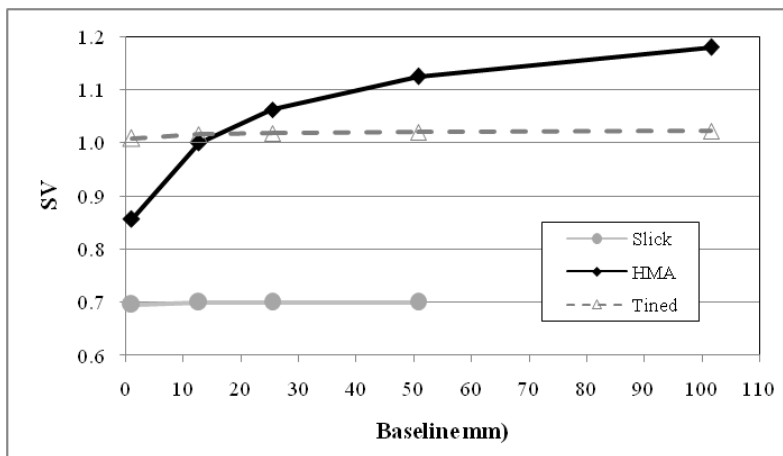
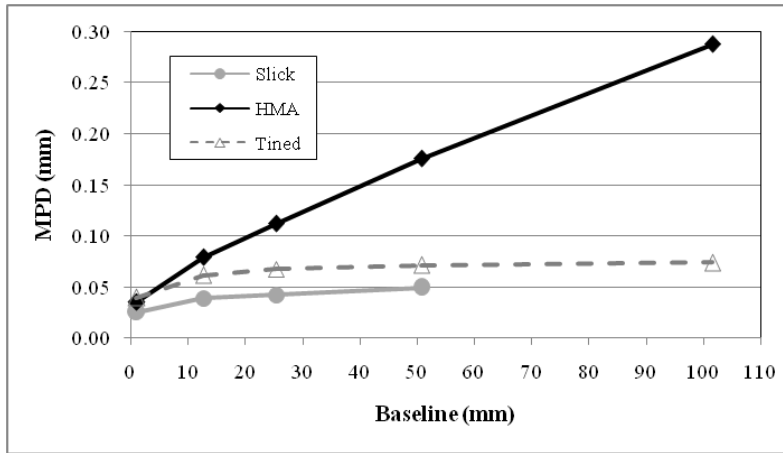


Figure 4-8 Variations of MPD, SV, and RMS with Baseline Length

It is shown that in general, MPD, SV, and RMS increase as the baseline length increases, regardless of the type of pavement surface. This is due to the fact that different baseline lengths may produce different regression lines. However, the increase rate decreases as the baseline length increases. It appears that all curves demonstrate a turning point with respect to the same baseline length of 12.75 mm (0.5 in.). The MPD, SV and RMS for the HMD surface increase more dramatically than those for the slick and tined concrete surface. Nevertheless, the increases are negligible for the slick and tined concrete surfaces, in particular when the baseline length is greater than 12.75 mm. In addition, the MPD, SV, and RMS associated with the HMA surface are more sensitive to the baseline length than those associated with both the slick and tined concrete surfaces. Generally speaking, increasing the baseline length invariably increases the MPD simply because a baseline of greater length provides greater possibility for greater texture depths to present according to the procedures of computation. However, the SV and RMS tend to remain more or less constant after the baseline length exceeds 12.75 mm. Therefore, a baseline of 12.75 mm may be a reasonable option in the computation of microtexture profile MPD, SV, and RMS.

Calculation of Microtexture MPD, SV and RMS

As pointed out earlier, the computation of MPD for the macrotexture profile is based on a baseline length twice the maximum wavelength of macrotexture, i.e., 100 mm (2 in.). Since the macrotexture and microtexture are the two dominant factors affecting pavement surface friction, it is advisable that the baseline length for evaluating microtexture be consistent to some extent with the baseline length for evaluating macrotexture. Taking into account the above considerations, it was recommended that in this study, the microtexture MPD, SV, and RMS should be computed in terms of a baseline length of 100 mm as follows:

- (1) Divide a 100-mm long microtexture profile into 8 equal, 12.75-mm long segments.
- (2) Compute the MPD_i , SV_i , and RMS_i for each segment ($i=1, 2, \dots, \text{and } 8$).
- (3) The MPD, SV, and RMS are respectively the average of MPD_i , SV_i , and RMS_i of the four segments.

Summarized in Table 4-4 are the MPD, SV, and RMS values computed in terms of the 12.75-mm baseline for the slick concrete, HMA, and tined concrete surfaces, respectively. The HMA surface demonstrates the greatest MPD. The reason is that while the average microtexture

depth on the HMA surface is 0.014 mm that is slightly less than that on the tined concrete surface, the variability of microtexture depth on the HMA surface is considerably greater than that on the tined concrete surface. A greater variability tends to produce a greater average difference between the microtexture profile and the regression line, resulting in a greater MPD. However, the tined concrete surface and the HMA surface have similar SV and RMS values. This indicates that in general, the HMA and tined concrete surfaces may have microtexture profiles with similar sharpness and asperity.

Table 4-4 The MPD, SV, and RMS in Terms of 12.75-mm Baseline

Surface	Slick Concrete	HMA	Tined Concrete
MPD (mm)	0.039	0.079	0.061
SV (mm)	0.700	1.000	1.016
RMS (mm)	0.013	0.021	0.021

POTENTIAL USE OF MICROTTEXTURE MEASUREMENTS IN ESTIMATING FRICTION

Pavement Friction Components

Based on Kummer's research work (5), the friction force can basically be determined by its two main components as follows:

$$F_{\mu} = F_a + F_h \dots\dots\dots(5-1)$$

where F_{μ} = friction force; F_a = adhesion force depending on the interface shear strength and the contact area; and F_h = hysteresis force component generated due to the damping losses within the rubber.

The formation of adhesion or hysteresis force depends on the surface condition. On a dry pavement, the friction force is dominated by the adhesion force if the surface is smooth and by the hysteresis force when the surface is rough. When water is present and pavement surface becomes lubricated, the adhesion force decreases and therefore the friction force decreases. Presented in Table 5-1 are the friction numbers measured on an in-service asphalt pavement (see Figure 5-1). The pavement surface was smooth and experienced no surface distresses, such as cracking and raveling. However, the exposed aggregates had been polished. In Table 5-1, the wet surface indicates that water was applied to the pavement surface before the beginning of applying brake. The dry surface indicates that no water was applied to the pavement in the entire process of testing.

Several observations can be made by examining the friction test results presented in Table 5-1. First, it is shown that under the dry condition, the smooth tire generated a friction number greater than that generated by the ribbed tire. This is because on the dry surface, the dominant friction force component is the adhesion force that is dependent on the contact area to a great extent. The contact area between the smooth tire and the pavement surface is much greater

than that between the ribbed tire and the pavement surface. Second, the friction numbers decreased dramatically when the pavement surface became wet. It decreased by roughly 71.0 for the smooth tire, and 41.1 for the ribbed tire. In other words, the adhesion force might be 71.0 for the smooth tire and 41.1 for the ribbed tire in this case. Since the hysteresis force became dominant when the surface was wet, the hysteresis force might be 36.5 for the ribbed tire and 27.2 for the smooth tire. This is probably because while the ribbed tire produced a smaller contact area, the contact pressure was high and caused more deformation in the rubber tire.

Table 5-1 Friction Numbers Measured on Wet and Dry Pavement

Surface Condition	Test Tire	Test Speed	Friction Number
Wet	Smooth	40 mph	27.2
Dry	Smooth	40 mph	98.2
Wet	Ribbed	40 mph	36.5
Dry	Ribbed	40 mph	77.6



Figure 5-1 Surface of the Tested Asphalt Pavement

Comparison of Texture and Friction Measurements

To investigate the possible use of texture measurements in estimating pavement friction, this study further conducted friction testing with the standard smooth tire on the INDOT friction

test track under dry and wet pavement conditions, respectively. Presented in Table 5-2 are the friction numbers measured at 30 mph. Under the dry pavement condition, the slick concrete surface provided the greatest friction number (FN) followed by the tined concrete surface. Under the wet pavement condition, however, the tined concrete surface produced the greatest FN followed by the HMA surface. The slick concrete surface produced the least FN. If the friction results in Table 5-1 and table 5-2 combined together, it is confirmed that on dry pavement, the adhesion force plays a critical role in the development of friction force when the surface is smooth. On the rough surface, the hysteresis force is consistently dominant no matter whether the pavement is wet or dry.

Table 5-2 Friction Numbers under Different Pavement Conditions

Pavement Surface Type	FN under Different Pavement Conditions		
	Wet	Dry	(FN _{Dry} -FN _{Wet})
Slick Concrete	10.8	89.3	78.5
9.5-mm HMA	44.6	84.6	40.0
Tined Concrete	71.5	88.4	16.9

Presented in Figures 5-2 and 5-3 are the variations of FN with macrotexture MPD and microtexture MPD, respectively. As shown in Figure 5-2, the wet pavement FN is proportional to the macrotexture MPD. As the macrotexture MPD increases, the dry pavement FN decreases slightly and then increases slightly, but appears slightly decreasing overall. This simply implies that wet pavement friction may be related to macrotexture and the effect of macrotexture on dry pavement friction is insignificant. On the contrary (see Figure 5-3), the dry pavement FN is inversely proportional to the microtexture MPD. As the microtexture MPD increases, the wet pavement FN decreases and then increases. This indicates that dry pavement friction may be related to microtexture and the effect of microtexture MPD on wet pavement friction depends on the microtexture MPD value. There may exist an optimum value of microtexture MPD. The wet pavement friction is proportional to the microtexture MPD that is less than the optimum value, and inversely proportional to the microtexture MPD that is greater than the optimum value. It is also shown that the FN difference is inversely proportional to the macrotexture MPD. While the FN difference decreases and then increases as the microtexture MPD increases, it appears decreasing on the whole.

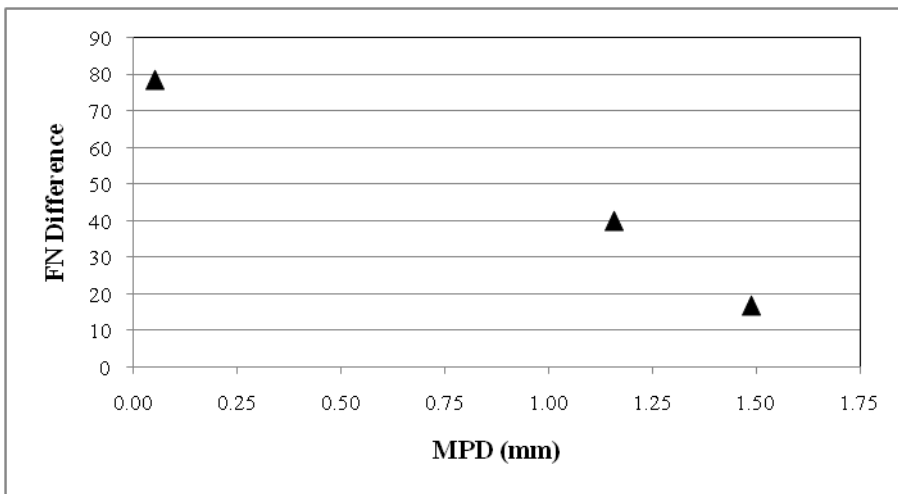
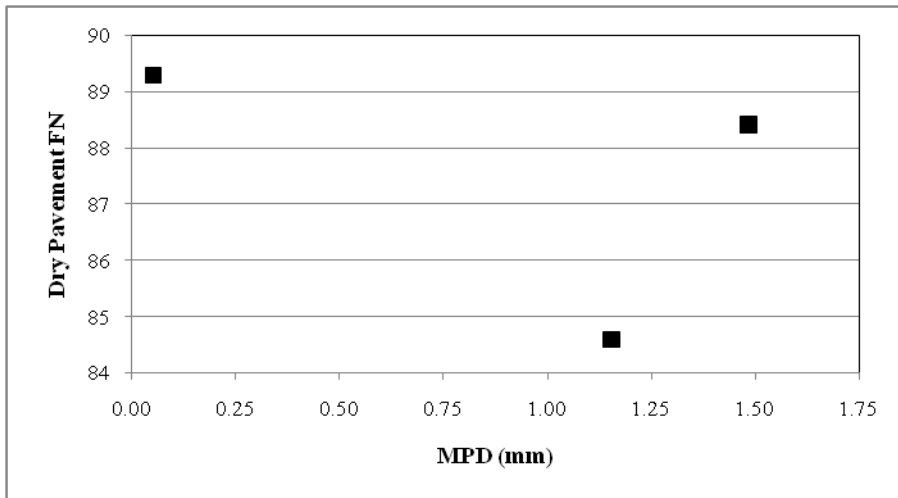
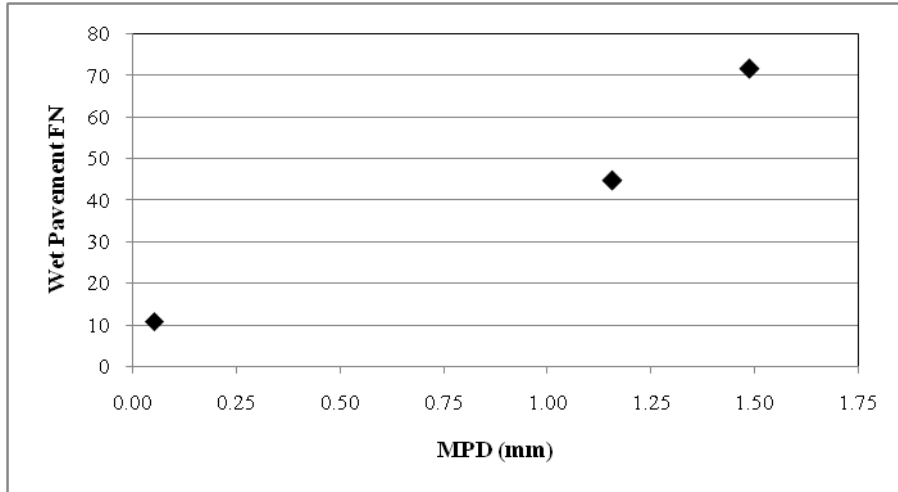


Figure 5-2 Variations of FN with Macrotexture MPD

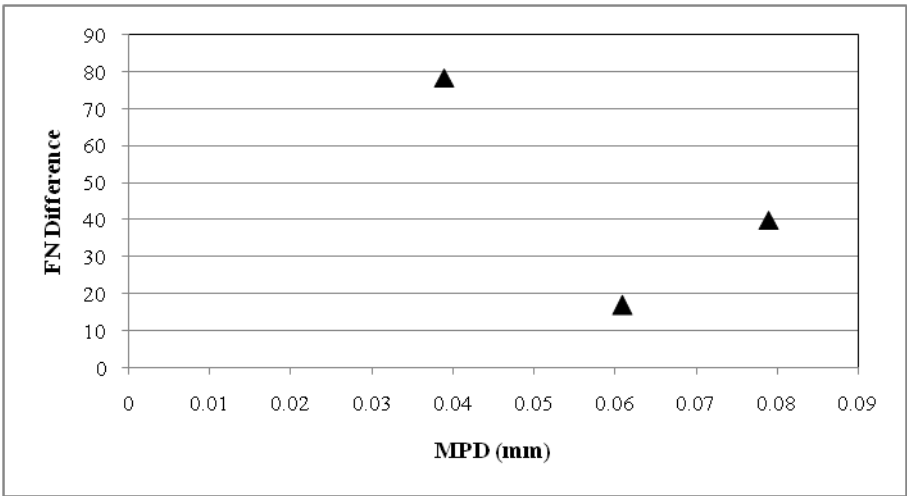
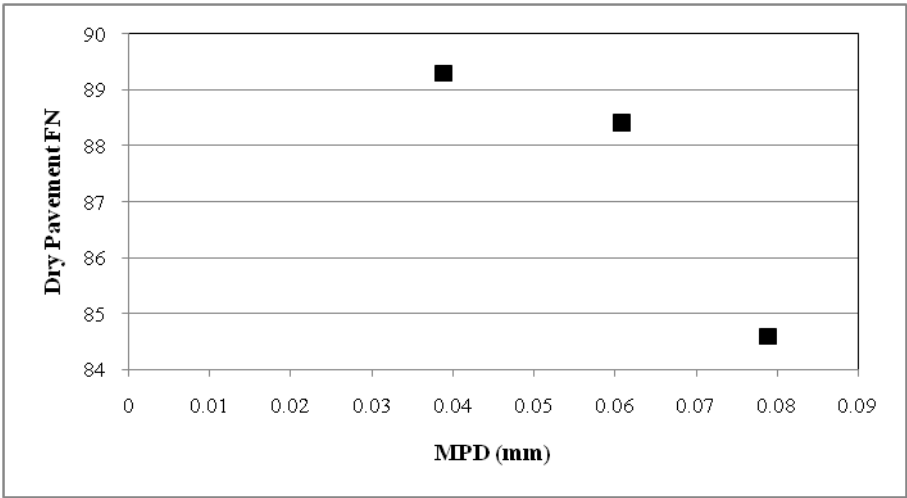
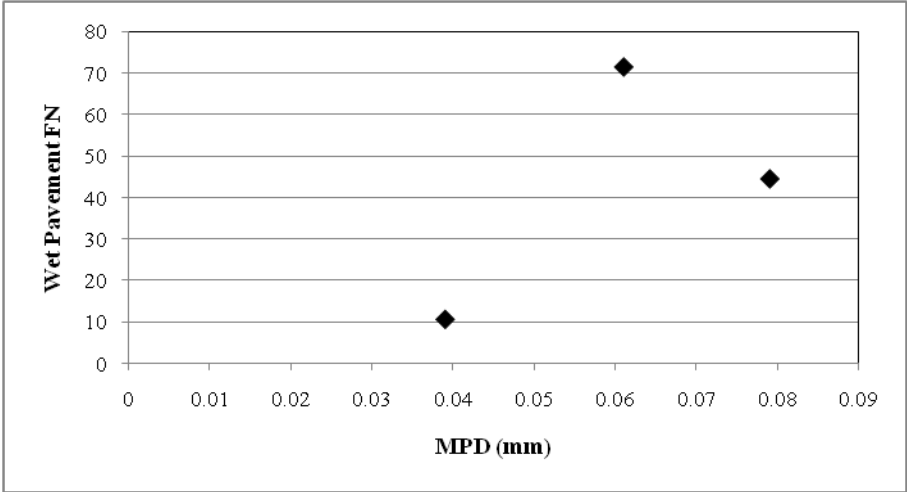


Figure 5-3 Variations of FN with Microtexture MPD

Plotted in Figure 5-4 are the variations of FN with microtexture SV and RMS, respectively. Careful inspection of the results in Figure 5-4 revealed that the variation of FN with RMS follows a trend very similar to that with SV. This can be expanded to conclude that while estimating friction from microtexture measurements, the use of SV (or sharpness) is as effective as the use of RMS (or asperity). Therefore, it is not necessary to include both SV and RMS when developing relationship between friction and microtexture measurements. Another observation made from Figure 5-4 is that the wet pavement FN is proportional to the microtexture SV. This indicates that the effect of microtexture on wet pavement friction is its SV value rather than its MPD value. As SV increases, the FN difference decreases.

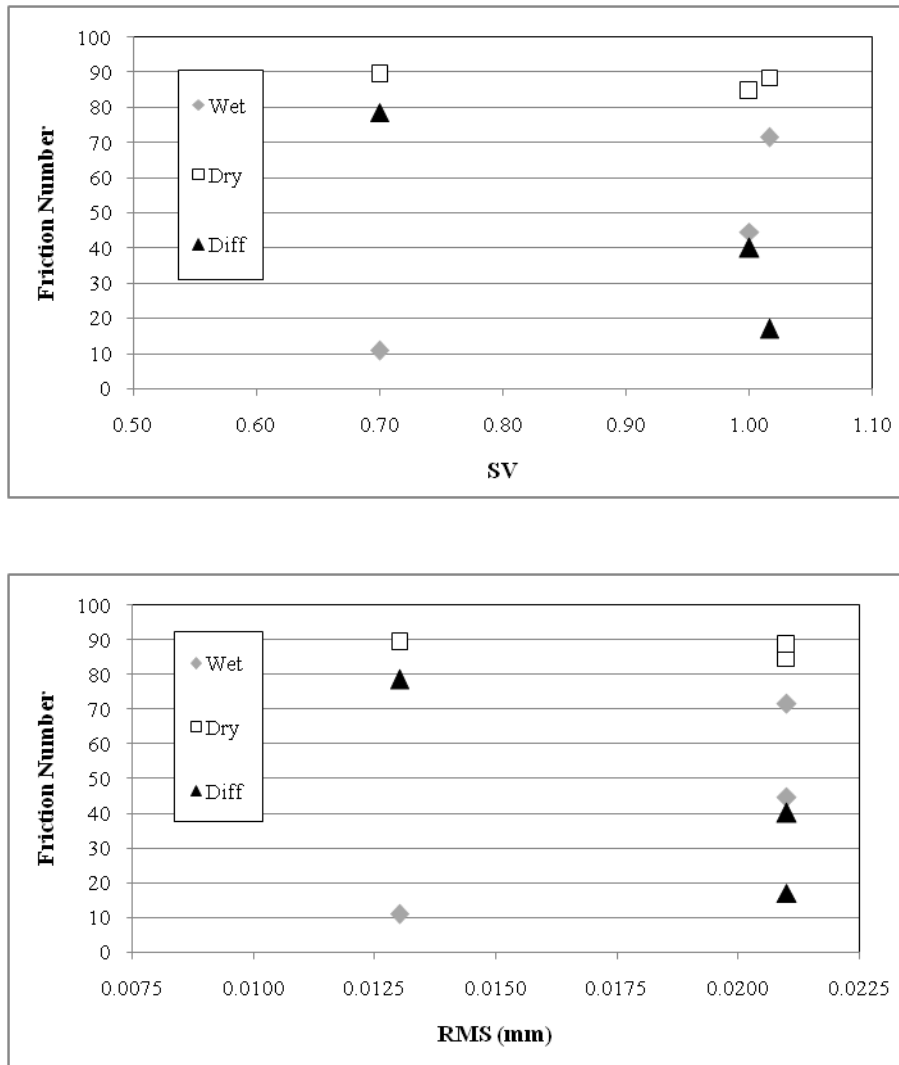


Figure 5-4 Variations of FN with Microtexture SV and RMS

Quantitative Relationship between Texture and Friction

Statistic analysis was conducted in this study to further investigate the quantitative relationships between pavement texture and friction measurements based on the data presented in Figures 5-2, 5-3, and 5-4. Two statistic tools, i.e., Pearson correlation procedures and linear regression procedures (9, 21), were employed in the process of statistic analysis. The Pearson correlation measures the dependence of two variables and is computed as the correlation coefficient by dividing the covariance of the two variables by the product of their standard deviations. The Pearson correlation coefficient equals +1 in the case of a perfect positive linear relationship, -1 in the case of a perfect negative linear relationship, and 0 when the two variables are independent. A Pearson correlation coefficient between -1 and +1 indicates the degree of linear association between the two variables. Linear regression often uses the least squares approaches to model the relationships between two or more variables.

Presented in Table 5-3 are the Pearson correlation coefficients between the friction and texture measurements on the three surfaces. Apparently, the wet pavement friction has a positive relationship with all three texture measurements, including macrotexture MPD, microtexture MPD, and microtexture SV. While the greatest degree of dependence occurred between the wet pavement FN and the macrotexture MPD, the wet pavement FN demonstrated great association with the microtexture in terms of SV. The correlation coefficient for the microtexture SV is much greater than that for the microtexture MPD. This indicates that the microtexture SV may play a more important role in the wet pavement friction than the microtexture MPD. On the dry pavement, the friction number has a negative relationship with all three texture measurements. The greatest degree of negative dependence arose between the FN and the microtexture MPD, and the least degree of negative dependence between the FN and the macrotexture MPD. This confirms that dry pavement friction is not as sensitive to macrotexture as to microtexture.

Table 5-3 Pearson Correlations between Friction and Texture Measurements

Friction Measurement	Texture Measurement		
	Macrotexture MPD	Microtexture MPD	Microtexture SV
Wet Pavement FN	0.9722	0.6026	0.9159
Dry Pavement FN	-0.4645	-0.9211	-0.6131

Presented below are the pavement friction prediction equations obtained using the linear regression procedures:

$$FN_{wet} = -11.425 + 38.133 \times MaMPD - 731.263 \times MiMPD + 69.714 \times MiSV \dots\dots(5-1)$$

$$FN_{dry} = 75.329 - 4.294 \times MaMPD - 259.221 \times MiMPD + 34.713 \times MiSV \dots\dots\dots(5-2)$$

where FN_{wet}=friction number on wet pavement, FN_{dry}=friction number on dry pavement, MaMPD=macrotexture MPD, MiMPD=microtexture MPD, and MiSV=microtexture SV.

The coefficient of determination is 1.0 for both Equation 5-1 and Equation 5-2. A coefficient of 1.0 indicates that there is a perfect correlation in the samples. It should be highlighted that caution should be exercised when using the above regression models due to two main reasons. First, the number of samples used in the regression analysis is not large enough to ensure necessary accuracy and reliability. Second, as mentioned in the preceding chapters, the 1-kHz laser used in this study is only capable of capturing microtextures having wavelengths of 0.03 mm to 0.5 mm. Therefore, not all microtexture information was included. However, two important inferences can be made from the above statistics analysis results. The first inference is that pavement friction is related to both macrotextrue and microtexture. The second inference is that when pavement is wet, its surface friction is more sensitive to the slope variance than to the mean profile depth of the microtexture profile.

CONCLUSIONS AND RECOMMENDATIONS

Conclusions

The selection of the laser measuring system depends not only on the texture waveband and amplitude, but also on the frequency of the texture profile. During field testing, the laser sensor system is mounted on a test vehicle and scans the pavement surface at the same speed as the vehicle. In other words, pavement texture profile can be considered as waves passing the laser at the speed of test vehicle. Therefore, the laser sampling frequency (f), pavement texture wavelength (λ), and vehicle speed (v) must follow the classic physics law, i.e., $f = v / \lambda$.

The laser's sampling frequency should meet the requirement by the Nyquist sampling theorem, which states that the sampling frequency should be at least twice the highest frequency contained in the signal. The real-life pavement texture usually consists of various wavelength components that produce different frequencies. The laser's sampling frequency should be at least twice the highest frequency associated with the shortest texture wavelength. To measure macrotextures with wavelengths of 0.5 mm to 50 mm, the required laser sampling frequency is 54 kHz at 30 mph and increases to 90 kHz at 50 mph. When measuring macrotextures with the 62.4 kHz laser, the effect of vehicle speed was not observed. When measuring macrotextures with the 1 kHz laser scanner, the effect of sunlight was observed.

In the calculation of macrotexture, the MPD values measured by the 1 kHz laser, 62.4 kHz laser, and the CTMeter demonstrated very good agreement on the tined concrete surface. On the 9.5-mm HMA surface, the MPD values measured by the 1 kHz laser and 62.5 kHz laser showed good agreement and are almost twice the MPD measured by the CTMeter. On the slick concrete surface, the MPD measured by the 62.5 kHz laser is considerably greater than those by the 1 kHz laser and the CTMeter. The MPD values measured by the 1 kHz laser and the CTMeter display noticeable difference, but are in the same order of magnitude. It was concluded that the 62.4 kHz laser is capable of capturing macrotexture on the tined concrete, and producing macrotexture data in good agreement with those by the 1 kHz laser on the 9.5-mm HMA surface.

Caution should be exercised when measuring macrotexture using the 62.4 kHz laser at high speeds.

The 62.5 kHz laser tended to produce a microtexture profile with spikes and troughs that are much greater than those measured by the 1 kHz laser. Only the microtexture data obtained using the 1 kHz laser scanner was used in the analysis. It was observed that the variations of microtexture depths are in a similar range regardless of the type of surface. It was also observed that a microtexture profile consisted of many wavelength or frequency components and the microtexture profile on the HMA surface demonstrated great variations probably due to the use of 27% of steel slag and 27% of dolomite in the aggregates. The measured microtexture depth was less than 0.05 mm on all the three surfaces. The tined concrete surface exhibited the greatest texture depth, and the slick concrete surface exhibited the smallest texture depth. The HMA surface demonstrates the greatest variability in microtexture depth.

Microtexture profile was composed of two categories of waves, i.e., large-scale and small-scale waves. The large-scale wave indicated the overall shape of the profile and the small-scale wave indicated the local roughness of the profile line, i.e., the deviations from the large-scale wave. For the large-scale waves, the largest wavelength was 0.475 mm on the tined concrete surface, 0.395 on the slick concrete surface, and 0.290 on the HMA surface. The average wavelength on the HMA surface was greater than those on both the slick and tined concrete surfaces.

Three variables, including MPD, SV and RMS, were employed to measure the characteristics of microtexture profile. It was found that these three variables increased as the baseline length increased, regardless of the type of pavement. However, the increase rate decreased as the baseline length increased, in particular when the baseline length exceeded 12.75 mm (0.5 in.). The MPD, SV and RMS for the HMD surface increased more dramatically than those for the slick and tined concrete surface. However, the SV and RMS tended to remain more or less constant after the baseline length exceeded 12.75 mm. It was recommended that the microtexture MPD, SV, and RMS should be computed in terms of a baseline length used for computing macrotexture. When estimating friction from microtexture measurements, the use of SV was as effective as the use of RMS. It is not necessary to include both SV and RMS when estimating friction from microtexture.

Pearson correlation analysis indicated that wet pavement friction had a positive relationship with all three variables, including macrotexture MPD, microtexture MPD, and microtexture SV. The greatest degree of dependence was associated with the macrotexture MPD, followed by the microtexture SV. The correlation coefficient for the microtexture SV was much greater than that for the microtexture MPD. The microtexture SV may play a more important role in wet pavement friction than the microtexture MPD. Dry pavement friction showed a negative relationship with the three variables. The greatest degree of negative dependence arose for the microtexture MPD, and the least degree of negative dependence for the macrotexture MPD. Therefore, dry pavement friction is not as sensitive to macrotexture as to microtexture.

Two inferences were made from the regression analysis. First, pavement friction is related to both macrotexture and microtexture, not to macrotexture only. Second, when pavement is wet, its surface friction is more sensitive to the slope variance than to the mean profile depth of the microtexture profile.

Recommendations

This pilot study systematically investigated the testing of pavement texture using the laser-based sensors and examined the correlations between pavement friction and texture. This study not only confirmed the findings reported by some researchers, but also brought the research one step closer to the goal of estimating pavement friction from texture measurements. Some work in this study is probably the first of its kind ever reported in literature. However, it should be recognized that more research work is needed to confirm the observations and findings obtained in this study, in particular those on microtexture testing and characterization. The shortcoming of this study is obviously associated with the capability of the 1 kHz laser used for measuring microtexture. The 1-kHz laser is capable of capturing textures having wavelengths of 0.03 mm to 50 mm, and some information on microtexture might be missing.

Three main recommendations have arisen due to the effort of this study. First, it was confirmed that wet pavement friction is related not only to macrotexture, but also to microtexture (in terms of the slope variance). To better relate pavement friction to texture, more research effort is needed to investigate the characterization of microtexture and examine the effect of macrotexture slope variance.

Second, while a laser system capable of capturing all microtextures is currently not commercially available, other no-contact sensing technologies, in particular the image processing, may have advanced to the point where a image processing system for measuring microtexture becomes feasible. Taking a commercial digital camera of 21 megapixels as an example, its pixel size is about 30 μm . The light that a commercial camera uses is usually visible light with wavelengths from 390 to 750 nm. Therefore, a sensor with a resolution of 30 μm and a wavelength of 390 to 750 nm is capable of capturing all microtextures. Research work is needed to examine the image processing technology for measuring microtexture.

Third, while the 1 kHz laser is not capable of capturing microtextures with wavelengths less than 0.03 mm, good correlations were observed between pavement friction and the microtexture measurements obtained using the 1 kHz laser. Therefore, it may be hypothesized that pavement friction is probably related to microtextures with wavelengths greater than a certain value. Research work is needed to confirm this hypothesis. If such a value exists, measuring microtexture using laser sensors at high speeds may become possible.

REFERENCES

1. ASTM Designation E 274-97, Standard Test Method for Skid Resistance of Paved Surfaces Using a Full-Scale Tire, Annual Book of ASTM Standards, Vol. 04. 03, 2001.
2. ASTM Designation E 501-94, Standard Specification for Standard Rib Tire for Pavement Skid-Resistance Tests, Annual Book of ASTM Standards, Vol. 04. 03, 2001.
3. ASTM Designation E 524-88 Standard Specification for Standard Smooth Tire for Pavement Skid-Resistance Tests, Annual Book of ASTM Standards, Vol. 04. 03, 2001.
4. ASTM Designation E 867-02a, Terminology Relating to Vehicle-Pavement System, Annual Book of ASTM Standards, Vol. 04. 03, 2002.
5. PIARC, Optimization of Pavement Surface Characteristics, PIARC Technical Committee on Surface Characteristics, Report to the XVIIIth World Road Congress, Brussels, Belgium, 1987.
6. Kummer, H. W., Unified Theory of Rubber and Tire Friction, Engineering Research Buletin B-94, The Pennsylvania State University, State College, 1966.

7. John J. Henry, Evaluation of Pavement Friction Characteristics, NCHRP Synthesis 291, Transportation Research Board, National Research Council, 2000.
8. ASTM Designation E 1845-01, Standard Practice for Calculating Pavement Macrotecture Mean Profile Depth, Annual Book of ASTM Standards, Vol. 04. 03, 2001.
9. Anthony J. Hayter. Probability and Statistics for Engineers and Scientists, 2nd Edition, Duxbury Press.
10. Bjarne Schmidt (2000). "Laser Texture Measurements of Asphalt Concrete," Nordic Road and Transport Research, No. 1, Danish Road Directorate.
11. Raymond A. Serway, and John W. Jewett (2005). Principles of Physics, 4th Edition, Thomson Brooks/cole, Belmont, CA94002.
12. Mu Xiangyang, Li Lin, Tang Nan, Ce Liu, and Jiang Xiuhan (2003). "Laser-Based System for Highway Pavement Texture Measurement," the Proceedings of the 2003 IEEE International Conference on Intelligent Transportation System, Vol. 2, 1559-1562.
13. Jiabin Xie, Richard Liu, and Brian Michalk (2008). "Automatic Skid Number Evaluation Using Texture Laser Measurements," IEEE International Conference on Networking, Sensing, and Control, April 6-8, 2008, Sanya, 37-42.
14. Steven W. Smith (1997). The Scientist and Engineer's Guide to Digital Signal Processing, California Technical Publishing, San Diego, CA 92150.
15. Ames Engineering (2008). Ames Engineering Laser Texture Scanner, User Manual, Software Version 6.0.
16. Mark Leichty (2010). The Laser Texture Scanner, Personal Email Communications, Ames Engineering (not published).
17. ASTM Designation E 2157-09, Standard Test Method for Measuring Macrotecture Properties Using the Circular Track Meter, Annual Book of ASTM Standards, Vol. 04. 03, 2009.
18. N. Mike Jackson, Bouzid Choubane, Charles Holzschuher, and Salil Gokhale (2007). "Measuring Pavement Friction Characteristics at Variable Speeds for Added Safety," American Society for Testing and Materials, STP 1486, 59-72.
19. Ames Engineering (2006). Ames Engineering Texture File Converter Software, User Manual, Software Version 1.0.

20. Richard Liu (2010). Personal Email Communication on Automatic Skid Number Evaluation Using Texture Laser Measurements (not published).
21. Statistix® 8 User's Manual, Analytical Software, Tallahassee, FL 32317.